



## DSMC simulation of subsonic flow through nanochannels and micro/nano backward-facing steps <sup>☆</sup>

Masoud Darbandi <sup>a,\*</sup>, Ehsan Roohi <sup>b</sup>

<sup>a</sup> Department of Aerospace Engineering, Institute for Nanoscience and Nanotechnology, Center of Excellence in Aerospace Systems, Sharif University of Technology, P. O. Box 11365-8639, Tehran, Iran

<sup>b</sup> Mechanical Engineering Group, Department of Engineering, Ferdowsi University of Mashhad, P.O. Box 91779-48974, Mashhad, Iran

### ARTICLE INFO

Available online 16 August 2011

#### Keywords:

DSMC  
Nanoflow  
Microflow  
Nanochannel  
Backward-facing step  
Subsonic flow

### ABSTRACT

In this study, we use direct simulation Monte Carlo method to simulate subsonic flow in nanochannels and micro/nanoscale backward-facing (BF) step considering a wide range of Knudsen number regimes. The nanochannel flow simulation indicates that the nanoscale flow through the nanochannel resembles unique features such as encountering negative pressure deviation behavior and observing flat velocity profiles at higher Knudsen number regimes. On the other hand, the micro/nano BF step flow simulations demonstrate that the length of separation region considerably decreases as the flow becomes more rarefied and approaches the transition regime. Meanwhile, the variations in the flow properties are much slower in the mid-transition and free-molecular regimes compared with the slip and early transition regime cases.

© 2011 Elsevier Ltd. All rights reserved.

### 1. Introduction

Fast progress in micro/nanoscale devices has drawn the attention of many workers to extend suitable numerical tools to analyze nanoscale flows through basic geometries, e.g., channels, backward-facing (BF) steps, and nozzles, more accurately. However, the flow in such scales can be rarefied. Indeed, Knudsen number is known as a key parameter to measure the gas rarefaction in micro/nano scales. It is defined as the ratio of mean free path of gas molecules,  $\lambda$ , to one characteristic dimension of flow,  $L$ , i.e.,  $Kn = \lambda/L$ . Using this definition, the non-rarefaction and rarefaction regimes can be categorized as no-slip ( $Kn < 0.01$ ), slip ( $0.01 < Kn < 0.1$ ), transition ( $0.1 < Kn < 10$ ), and free-molecular ( $Kn > 10$ ) ones. Based on the past experiences, the Navier–Stokes (NS) equations have been largely used to simulate the non-rarefied flows through basic macro-scale geometries subject to the classical no-slip boundary conditions [1–3] and the rarefied flows through basic micro/nano-scale geometries subject to the velocity slip and temperature jump boundary conditions [4–10]. However, the resulting inaccuracies in the latter cases are high enough to promote the researchers to use the kinetic-based approaches such as the direct simulation Monte Carlo (DSMC) method [11] in treating highly rarefied flows. As is known, DSMC is capable of solving flow for a wide range of rarefaction regimes with sufficient accuracies [12]. Bao and Lin [13] used the continuum-based Burnett equations and simulated the microscale

BF step flows at transition regime. Their results were in good agreement with the DSMC solution; however, if  $Kn < 0.5$ .

Literature shows that DSMC has been widely applied to simulate rarefied flows through the aforementioned basic geometries since many years ago. Beskok [14] used the DSMC solution to validate the accuracy of high order slip velocity boundary conditions in predicting BF step flows. Xue and Chen [15] and Xue et al. [16] used DSMC and simulated micro BF step flows in slip and transition regimes. Their results showed that the flow separation and recirculation, which are two main characteristics of the BF step flow in macroscales, would disappear if  $Kn > 0.1$ . Agrawal et al. [17] simulated the rarefied slip flow regime in microchannels with sudden expansion or contraction using the Lattice Boltzmann method. Zhen et al. [18] used 2D and 3D DSMC calculations to evaluate heat transfer in short microchannels. Wang et al. [19,20] used DSMC and studied the flow and heat transfer behavior in microchannels with constant wall heat flux boundary condition. Roohi et al. [21] used DSMC and simulated the subsonic flow through micro/nanoscale channels. They studied the effects of different wall thermal boundary conditions on the flow field behavior. Gatsonis et al. [22] used an unstructured DSMC solver to study supersonic flow in 3D nanochannels. Hsieh et al. [23] used the DSMC and solved the flow through 3D microscale BF step. They indicated that the approaching level of 3D flows to 2D simplifications would be over 98% for the flow with an inlet Knudsen number of 0.041. The approaching level decreased as  $Kn$  increased. They also reported that the flow separation, recirculation, and reattachment would disappear as the cross-section aspect ratio became less than unity. Darbandi and Roohi [24] used an unstructured DSMC solver and studied the subsonic and supersonic flows in micro/nanoscale converging–diverging nozzles. They reported that the mixed impacts of rarefaction,

<sup>☆</sup> Communicated by W.J. Minkowycz.

\* Corresponding author at: Sharif University of Technology, Azadi Ave., P. O. Box 11365-8639, Tehran, Iran.

E-mail address: [darbandi@sharif.edu](mailto:darbandi@sharif.edu) (M. Darbandi).

compressibility, and viscous forces would form the flow behavior in the micro/nanoscale nozzles.

The objective of this work is to provide a deeper understanding of subsonic flow in nanoscale channels and the micro/nanoscale BF steps. Indeed, past researchers, e.g., Refs. [15–17], do not sufficiently focus on the physics of flow field in nanoscale geometries. The current nanochannel flow simulation demonstrates some unique behavior, e.g., a negative pressure deviation from the linear distribution, which was not reported elsewhere. Additionally, we show that the flow field variation decreases as the Knudsen number increases in transition regime.

The rest of this paper is organized as follows. Section 2 briefly describes the DSMC method and the required subsonic boundary condition implementation. Section 3 presents the results for the rarefied flow through nanochannels and micro/nanoscale BF steps. The concluding remarks are provided in Section 4.

## 2. The DSMC algorithm

DSMC is a numerical tool to solve the Boltzmann equation based on the direct statistical simulation of the molecular processes described by the kinetic theory. The primary principle of DSMC is to decouple the motion and collision of particles during one time step. The implementation of DSMC needs breaking down the computational domain into a collection of grid cells. The cells are divided into sub-cells in each direction. These sub-cells are then utilized to facilitate the selection of collision pairs. After fulfilling all the molecular movements, the collisions between particles are simulated using Variable Hard Sphere (VHS) collision model and Larsen–Borgnakke internal energy redistribution model [11]. The values of mass flow rate at the inlet and outlet are monitored until there is no difference between the inlet and outlet mass flow rates. After achieving steady flow condition, sampling of molecular properties is fulfilled within each cell during a sufficient large time step to avoid any types of statistical scattering. All thermodynamic parameters such as temperature, density, and pressure are then obtained from these time-averaged data. The required time step length is calculated such that the CFL number, based on the most probable speed,  $CFL = V_{mp} dt/dx$ , remains less than 0.2. The time step size should also be a fraction of the mean collision time of the gas molecules, i.e.,  $dt < \lambda/V_{mp}$ .

The current authors have already developed different 2D and 3D DSMC solvers to simulate rarefied flow in microscale and nanoscale geometries [12,21,24] and hypersonic regimes [25]. In this study, we use our solver to simulate the rarefied flow through nanochannels and micro/nano scale BF steps. The results are presented shortly.

### 2.1. Subsonic boundary condition

For a subsonic pressure driven flow, the outlet pressure is known. We use the 1-D characteristic theory to apply the inlet/outlet pressure boundary conditions [26]. For a backward-running wave, we consider  $du/a = -d\rho/\rho$ , where  $a = \sqrt{dp/d\rho}$  is the speed of sound and  $p$  and  $\rho$  represent pressure and density, respectively. Applying the differential definition of  $a$  to a boundary cell, the outlet density is calculated from

$$(\rho_o)_j = \rho_j + \frac{p_o - p_j}{a_j^2} \quad (1)$$

The subscripts  $o$  and  $j$  represent the quantities at the outlet and the  $j$ th cell adjacent to the outlet boundary, respectively. Using the equation of state, the temperature can be found at the outlet using

$$(T_o)_j = \frac{p_o}{(\rho_o)_j R} \quad (2)$$

Using the characteristic wave equation, the velocity is also computed from

$$(u_o)_j = u_j + \frac{p_j - p_o}{\rho_j a_j} \quad (3)$$

For a subsonic pressure driven flow, the inlet velocity is also unknown and must be extrapolated from the interior domain. The inlet velocity is calculated from

$$(u_{in})_j = u_j + \frac{p_{in} - p_j}{\rho_j a_j} \quad (4)$$

The density at the inlet is calculated from the equation of state as follows:

$$(\rho_{in})_j = \frac{p_{in}}{RT_{in}} \quad (5)$$

## 3. Results and discussion

We apply the extended DSMC solver to analyze the rarefied subsonic flows through two basic nanochannel and BF step geometries in micro/nanoscales.

### 3.1. Subsonic flow through nanochannels

We study different nanochannel cases in order to elaborate the nanoflow behavior in subsonic regimes. They are summarized in Table 1. We simulate only one half of channel due to the symmetry for both geometry and flow. Cases 1–3 are in transition regime and Case 4 is in the mixed transition-free-molecular regime. Fig. 1(a) typically shows the convergence of mass flow rate at the inlet and outlet of nanochannel for Case 2. This figure also shows the convergence history of the implicitly applied inlet/outlet pressure boundary conditions. It is worth no mention that we continued our simulation even after meeting the defined convergence criterion. Helped us to suppress the statistical DSMC errors more effectively. We also performed a grid independency activity to finalize the suitable grid sizes in our simulations. Fig. 1(b) shows the pressure distributions achieved for Case 2 using Grid 1 ( $50 \times 15$  cells), Grid 2 ( $100 \times 30$  cells), and Grid 3 ( $150 \times 45$  cells). It is observed that all three grids provide similar pressure distributions or centreline pressure solutions. Therefore, we continue our study using Grid 2. We set 25–30 molecules in each cell at time zero.

Fig. 2(a) shows the pressure distribution along the nanochannel centreline for Cases 2–4. Two important points can be concluded from this figure. First, an increase in Knudsen number would result in a

**Table 1**  
Numerical tests performed to study subsonic flow through nanochannels.

Case	1	2	3	4
Gas	N <sub>2</sub>			
h(nm)	21	39.2	15.2	2.3
AR (L/h)	10	10	10	10
Kn <sub>in</sub>	1	0.25	0.6	6
Kn <sub>out</sub>	2.5	0.75	1.8	18
M <sub>in</sub>	0.08	0.025	0.025	0.025
M <sub>out</sub>	0.26	0.086	0.086	0.086
Grid	100 × 30	100 × 30	100 × 30	100 × 30
P <sub>b</sub> (KPa)	97.5	66.6	66.6	66.6
P <sub>in</sub> (KPa)	243.5	200	200	200
Pressure Ratio	2.5	3	3	3
T <sub>wall</sub> (K)	300	300	300	300
Re <sub>in</sub>	0.104	0.040	0.033	0.003

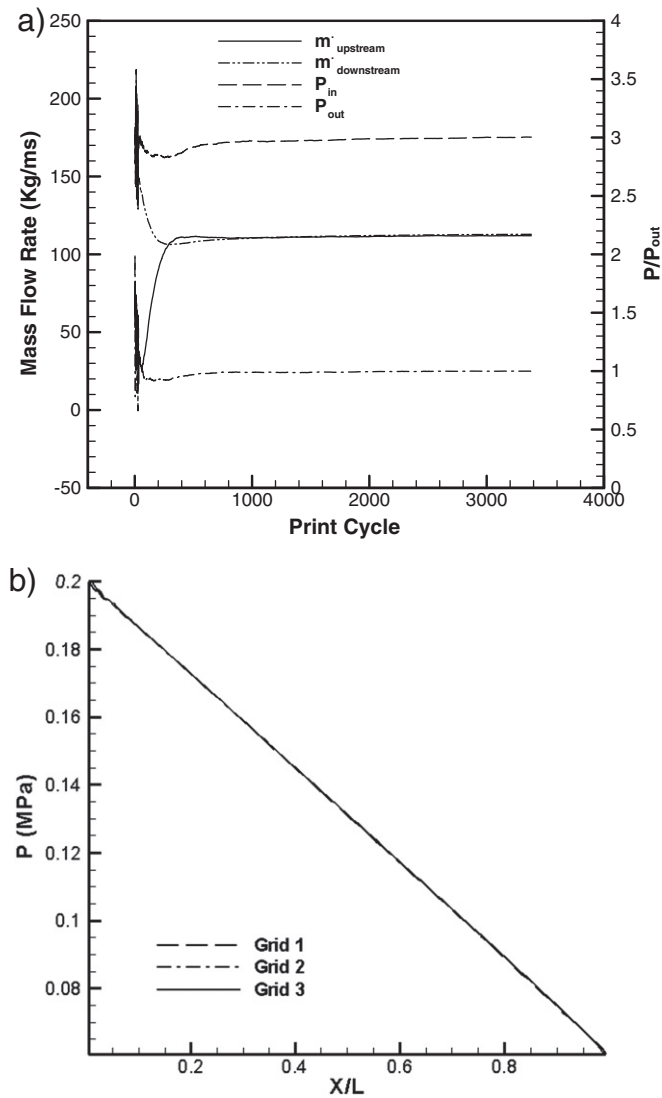


Fig. 1. a) Convergence of mass flow rate and inlet/outlet pressures, b) grid independency study, Case 2.

decrease in the slope of pressure distribution. Second, the rate of pressure slope reduction decreases as the Knudsen number increases. For example, the inlet Knudsen number increases from 0.25 to 0.6 for Cases 2 and 3 and from 0.6 to 6 for Cases 3 and 4. Furthermore, the variations in the pressure distribution slope are more visible from Case 2 to Case 3 than those from Case 3 to Case 4. We can conclude that the variations in the flow behavior would decrease as the Knudsen number approaches the upper limit of transition regime.

Fig. 2(b) shows the pressure deviation from the linear incompressible distribution for Cases 2–4. Case 2 performs the highest deviation compared with those of other two cases. As is seen, the pressure deviation is almost zero for Case 3, indicating that the pressure distribution is almost linear in this case. It should be noted that the compressibility and rarefaction are two key factors, which affect the pressure distribution differently and adversely. In other words, compressibility increases the pressure nonlinearity while the rarefaction causes more linearity for the pressure distribution. These two factors balance their impacts in Case 3. Therefore, pressure distribution is almost linear in this case. As the Knudsen number increases in Case 4, the rarefaction effect becomes more dominant

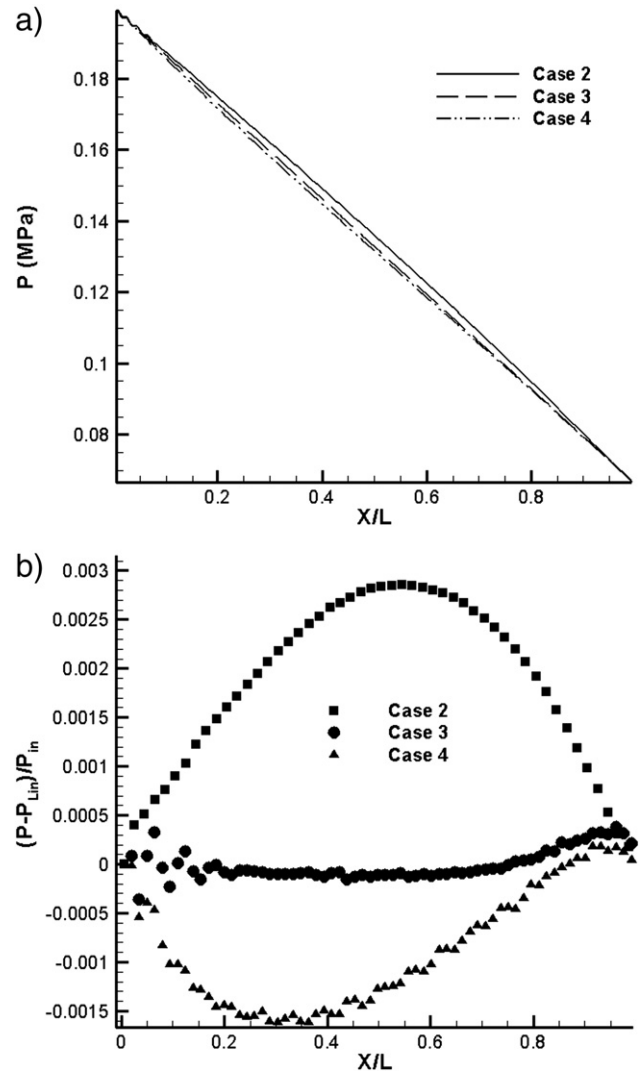


Fig. 2. The nanochannel results for Cases 2–4, a) the pressure distribution along the centreline, b) deviation of centreline pressure distribution from the linear one.

than the compressibility effect. Consequently, the pressure deviation from the incompressible distribution is almost negative for this case.

Fig. 3 shows the velocity profiles at different locations ( $X/L = 0.4, 0.6, \text{ and } 0.8$ ) for Cases 3 and 4. The velocity profiles are normalized using the slip velocity magnitude. As the Knudsen number increases, the slip velocity increases along the nanochannel walls and the ratio of centreline velocity to the slip velocity decreases. Consequently, the non-dimensional velocity variation decreases in the channel in the mid transition and free-molecular regimes. In other words, the velocity profiles are flattened more using dimensional scales.

### 3.2. Flow in nano/micro backward-facing step

The next is to study the rarefied flow through BF step considering different Knudsen numbers. We set the pressure ratio along the channel equal to 2 and specify the wall and inlet gas temperatures at 300 K. We use a grid with  $100 \times 60$  structured cells and set 25 particles in each cell. We perform our simulations for different Kn numbers in slip, transition, and free-molecular regimes. Fig. 4 shows the Mach number contours imposing different inlet Knudsen numbers. The BF

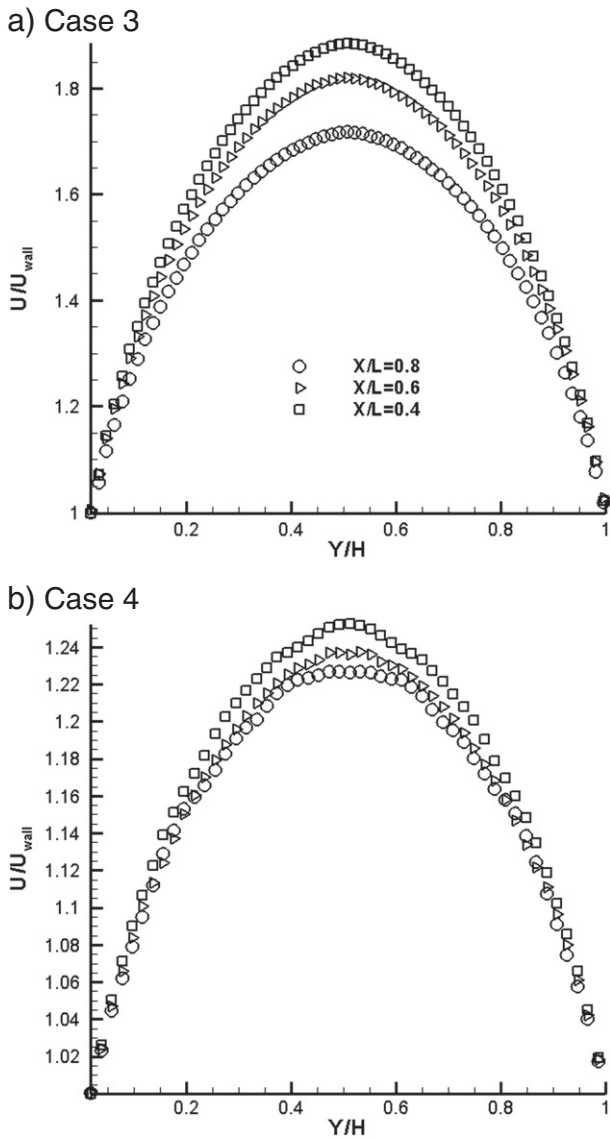


Fig. 3. Velocity profiles at different locations across the nanochannel.

step height is equal to the channel inlet height. The other lengths in this figure are non-dimensionalized with the BF step height. As is seen, the maximum separation length is for the slip flow case having

$Kn = 0.01$ . However, it is observed that the length of separation region slightly decreases as the flow  $Kn$  number increases from the top limit of slip flow regime ( $Kn = 0.10$ ) to the low limit of free-molecular regime ( $Kn = 10.0$ ). The first reason for this phenomenon is the decrease of Reynolds ( $Re$ ) number with the increase of  $Kn$  number. As the  $Re$  number decreases, the viscous forces become more dominant and consequently the length of separated region would decrease. The second reason is attributed to the rarefaction effects, which causes the velocity slip at the walls. Therefore, the flow adjacent to wall gets a lower chance of separation.

Fig. 5 shows the Mach number and pressure distributions at different  $Y/S$  levels such as the top wall (TW), the centreline (CL), the bottom wall (BW) and  $Y/S = 0.25$  and  $0.45$ . It is observed that the variations of Mach number and pressure magnitudes are much higher at lower  $Kn$  numbers. For all cases, the maximum Mach number occurs at the mid-height level. There is a jump (discontinuity) in pressure and Mach number right at the beginning of BF step. We observe that the pressure increases along the separated region for  $Kn = 0.01$ . As the length of separated region decreases at higher  $Kn$  number values, the increase in pressure is restricted to a smaller region. Meanwhile, the jump in pressure value increases as the  $Kn$  number increases from  $0.01$  to  $0.1$  but it is almost constant for  $Kn = 1$  and  $10$  regimes. Before the BF step region and as soon as the separation region ends up, the pressure starts slowing down similar to the case where the flow passes through a constant area channel [14].

4. Conclusion

We used DSMC algorithm and simulated subsonic flow in nanochannels and micro/nanoscale BF steps considering a wide range of rarefaction regimes. In simulating the low speed subsonic flow through the nanochannels, we observed that the pressure distribution along the channel deviates from a linear distribution as soon as the Knudsen number reaches the early free-molecular regime. This can be attributed to the rarefaction increase, which dominates the compressibility effects and makes the pressure deviation more negative. In the free-molecular regime, the slip velocity over the wall increases in a manner that the variation of non-dimensional velocity profile decreases along the channel. The simulations of micro/nano BF step flow demonstrate that the length of separation region considerably decreases as the flow influences more in the transition regime region. However, the variations in the flow properties are much slower in the mid-transition and free-molecular regimes compared with the slip and early transition regimes.

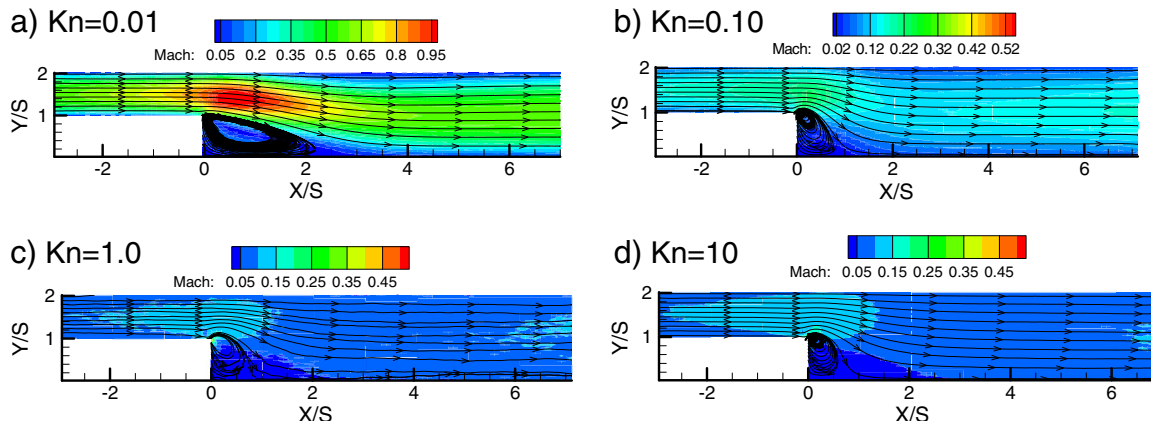


Fig. 4. Mach number contours in BF step flow using different Knudsen numbers, ( $S \equiv$  BFS height).

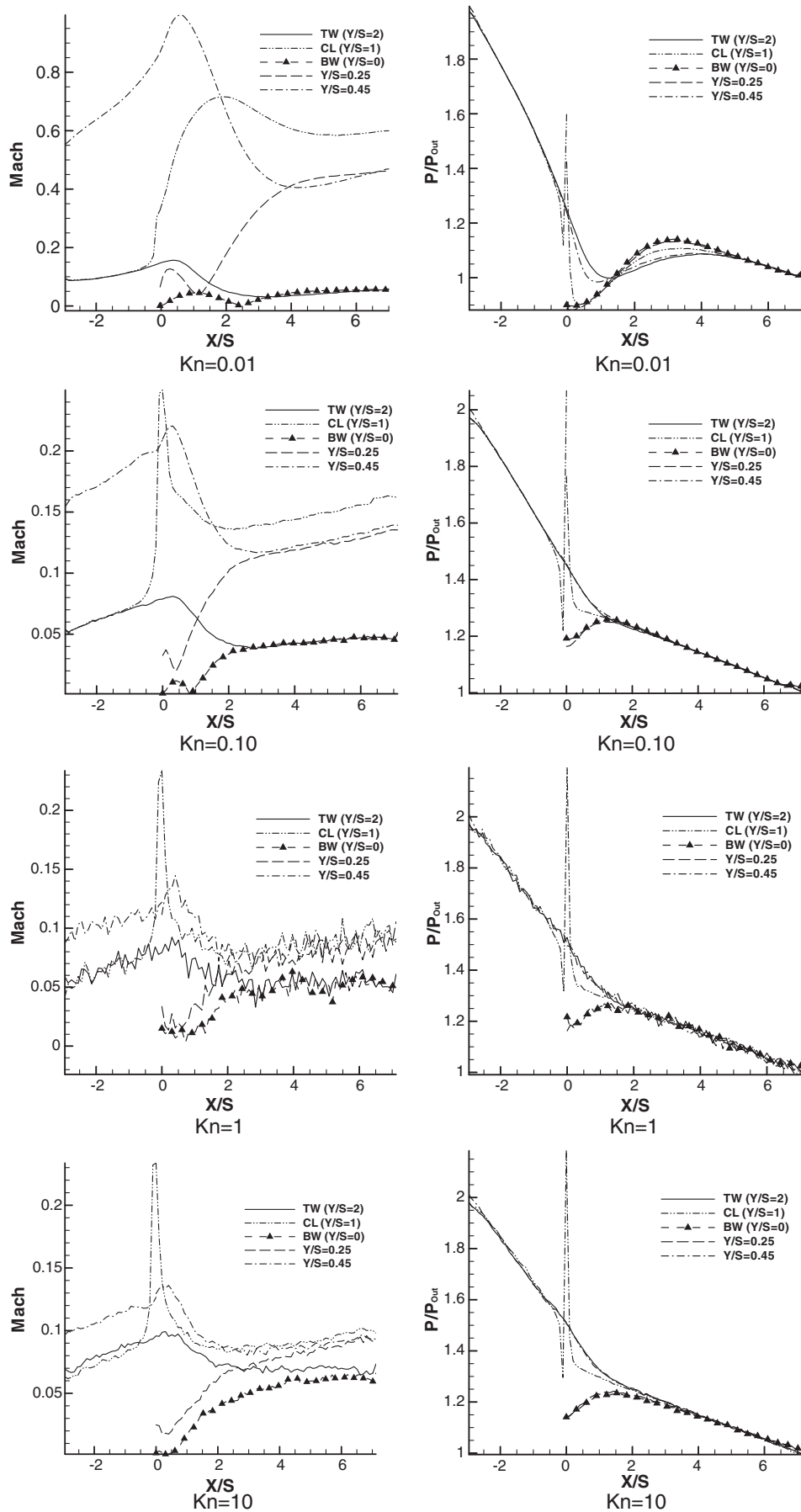


Fig. 5. Mach number and pressure distributions at different heights of the BF step considering various Knudsen number magnitudes.

## References

- [1] M. Darbandi, G.E. Schneider, Application of an all-speed flow algorithm to heat transfer problems, *Numerical Heat Transfer, Part A: Applications* 35 (7) (1999) 695–715, doi:10.1080/104077899274985.
- [2] P. Rajesh Kanna, M.K. Das, Heat transfer study of two-dimensional laminar incompressible wall jet over backward-facing step, *Numerical Heat Transfer, Part A: Applications* 50 (2) (2006) 165–187.
- [3] M. Darbandi, M. Taeibi-Rahni, A.R. Naderi, Firm structure of the separated turbulent shear layer behind modified backward-facing step geometries, *International Journal of Numerical Methods for Heat & Fluid Flow* 16 (7) (2006) 803–826, doi:10.1108/09615530610683520.
- [4] H.P. Kavehpour, M. Faghri, Y. Asako, Effects of compressibility and rarefaction on gaseous flows in microchannels, *Numerical Heat Transfer, Part A: Applications* 32 (7) (1997) 677–696.
- [5] H. Sun, M. Faghri, Effects of Rarefaction and compressibility of gaseous flow in microchannel using DSMC, *Numerical Heat Transfer, Part A: Applications* 38 (2) (2000) 153–168.
- [6] H. Choi, D. Lee, J.S. Maeng, Computation of slip flow in microchannels using Langmuir slip condition, *Numerical Heat Transfer, Part A: Applications* 44 (1) (2003) 59–71.
- [7] M. Darbandi, S. Vakilipour, Developing consistent inlet boundary conditions to study the entrance zone in microchannels, *Journal of Thermophysics and Heat Transfer* 21 (3) (2007) 596–607.
- [8] S. Vakilipour, M. Darbandi, Advancement in numerical study of gas flow and heat transfer in microchannels, *Journal of Thermophysics and Heat Transfer* 23 (1) (2009) 205–208.
- [9] Z. Sun, Y. Jaluria, Numerical modeling of pressure-driven nitrogen slip flow in long rectangular microchannels, *Numerical Heat Transfer, Part A: Applications* 56 (7) (2009) 541–562.
- [10] S. Bigham, H. Shokouhmand, R.N. Isfahani, S. Yazdani, Fluid flow and heat transfer simulation in a constricted microchannel: effects of rarefaction, geometry, and viscous dissipation, *Numerical Heat Transfer, Part A: Applications* 59 (3) (2011) 209–230.
- [11] G.A. Bird, *Molecular Gas Dynamics and the Direct Simulation of Gas Flows*, Clarendon, Oxford, 1994.
- [12] E. Roohi, M. Darbandi, Extending the Navier–Stokes solutions to transition regime in two-dimensional micro-/nanochannel flows using information preservation scheme, *Physics of Fluids* 21 (2009) 082001.
- [13] F. Bao, J. Lin, Continuum simulation of the microscale backward-facing step flow in a transition regime, *Numerical Heat Transfer, Part A: Applications* 59 (8) (2011) 616–632.
- [14] A. Beskok, Validation of a new velocity-slip model for separated gas microflows, *Numerical Heat Transfer, Part B* 40 (6) (2001) 451–471.
- [15] H. Xue, S.H. Chen, DSMC simulation of microscale backward-facing step flow, *Nanoscale Microscale Thermophysical Engineering* 7 (1) (2003) 69–86.
- [16] H. Xue, B. Xu, Y. Wei, J. Wu, Unique behaviors of a backward-facing step flow at microscale, *Numerical Heat Transfer, Part A* 47 (2005) 251–268.
- [17] A. Agrawal, L. Djenidi, R.A. Antonia, Simulation of gas flow in microchannels with a sudden expansion or contraction, *Journal of Fluid Mechanics* 530 (2005) 135–144.
- [18] C.E. Zhen, Z.C. Hong, Y.J. Lin, N.T. Hong, Comparison of 3-D and 2-D DSMC heat transfer calculations of low-speed short microchannel flows, *Numerical Heat Transfer, Part A: Applications* 52 (3) (2007) 239–250.
- [19] Q.W. Wang, C.L. Zhao, M. Zeng, Y.M. Wu, Numerical investigation of rarefied diatomic gas flow and heat transfer in a microchannel using DSMC with uniform heat flux boundary condition—Part I: Numerical method and validation, *Numerical Heat Transfer, Part B*: 53 (2) (2008) 160–173.
- [20] Q.W. Wang, C.L. Zhao, M. Zeng, Y.M. Wu, Numerical investigation of rarefied diatomic gas flow and heat transfer in a microchannel using DSMC with uniform heat flux boundary condition—Part II: Applications, *Numerical Heat Transfer, Part B* 53 (2) (2008) 174–187.
- [21] E. Roohi, M. Darbandi, V. Mirjalili, DSMC solution of subsonic flow through micro-nano scale channels, *Journal of Heat Transfer* 131 (9) (2009) 092402.
- [22] N. Gatsonis, W. Al-Kouz, R. Chamberlin, Investigation of rarefied supersonic flows into rectangular nanochannels using a three-dimensional direct simulation Monte Carlo method, *Physics of Fluids* (22) (2010) 032001.
- [23] T.Y. Hsieh, Z.C. Hong, Y.C. Pan, Flow characteristics of three-dimensional microscale backward-facing step flows, *Numerical Heat Transfer, Part A: Applications* 57 (5) (2010) 331–345.
- [24] M. Darbandi, E. Roohi, Study of supersonic-subsonic gas flows through micro-nano scale nozzles using unstructured DSMC solver, *Microfluids and Nanofluids Journal* 10 (2) (2011) 321–335.
- [25] T. Scanlon, E. Roohi, C. White, M. Darbandi, J. Reese, An open source, parallel DSMC code for rarefied gas flows in arbitrary geometries, *Computers and Fluids* 39 (2010) 2078–2089.
- [26] M. Wang, Z. Li, Simulations for gas flows in microgeometries using the direct simulation Monte Carlo method, *International Journal of Heat and Fluid Flow* (25) (2004) 975–985.